



Universiteit
Leiden
The Netherlands

Immune evasion by varicelloviruses : the identification of a new family of TAP-inhibiting proteins

Koppers-Lalić, D.

Citation

Koppers-Lalić, D. (2007, September 11). *Immune evasion by varicelloviruses : the identification of a new family of TAP-inhibiting proteins*. Retrieved from <https://hdl.handle.net/1887/12381>

Version: Corrected Publisher's Version

License: [Licence agreement concerning inclusion of doctoral thesis in the Institutional Repository of the University of Leiden](#)

Downloaded from: <https://hdl.handle.net/1887/12381>

Note: To cite this publication please use the final published version (if applicable).

CHAPTER

6

J Virol. 2006; 80:5822-5832

Bovine Herpesvirus 1 UL49.5 Protein Inhibits the Transporter Associated with Antigen Processing despite Complex Formation with Glycoprotein M

Andrea D. Lipińska^{1,2}, Danijela Koppers-Lalic¹, Michał Rychłowski², Pieter Admiraal¹, Frans A. M. Rijsewijk³, Krystyna Bieńkowska-Szewczyk² and Emmanuel J. H. J. Wiertz¹

¹ Department of Medical Microbiology, Leiden University Medical Center, 2300 RC Leiden

² Department of Molecular Virology, University of Gdańsk, 80-822 Gdańsk, Poland

³ Virus Discovery Unit, Animal Sciences Group, 8200 AB Lelystad, 3 The Netherlands,

Bovine herpesvirus 1 (BHV-1) interferes with peptide translocation by the transporter associated with antigen processing (TAP). Recently, the UL49.5 gene product of BHV-1 was identified as the protein responsible for the observed inhibition of TAP. In BHV-1-infected cells and virions, the UL49.5 protein forms a complex with glycoprotein M (gM). Hence, it was investigated whether UL49.5 can combine the interactions with gM and the TAP complex. In cell lines constitutively expressing both UL49.5 and gM, UL49.5 appears to be required for functional processing of gM. Immunofluorescence-confocal laser scanning microscopy demonstrated that both proteins are interdependent for their redistribution from the endoplasmic reticulum to the *trans*-Golgi network. Remarkably, expression of cloned gM results in the abrogation of the UL49.5-mediated inhibition of TAP and prevents the degradation of the transporter. However, in BHV-1-infected cells, differences in UL49.5 and gM expression kinetics were seen to create a window of opportunity at the early stages of infection, during which time the UL49.5 protein can act on TAP without gM interference. Moreover, in later periods, non-gM-associated UL49.5 can be detected in addition to the UL49.5/gM complex. Thus, it has been deduced that different functions of UL49.5, editing of gM processing and inhibition of TAP, can be combined during BHV-1 infection.

Bovine herpesvirus 1 (BHV-1) belongs to the subfamily *Alphaherpesvirinae* and the genus *Varicellovirus*. BHV-1 infections affect the respiratory tract, the eyes, and the reproductive tract of cattle (9). BHV-1 downregulates the cell surface expression of major histocompatibility complex (MHC) class I molecules to evade recognition by host cytotoxic T cells (10, 19). Recently, it was demonstrated that the product of the BHV-1 UL49.5 gene blocks the transporter associated with antigen processing (TAP) (18). The TAP complex consists of two subunits, TAP1 and TAP2, and is combined with MHC class I molecules and several other accessory molecules in the MHC class I peptide-loading complex (5, 37). TAP translocates antigenic peptides from the cytosol into the endoplasmic reticulum, where they are loaded onto newly synthesized MHC class I molecules. TAP thus mediates an essential function in the MHC class I antigen presentation pathway (5, 37). Cells expressing UL49.5 show a strongly reduced MHC class I surface expression and demonstrate a severely impaired capacity to activate cytotoxic T cells (18).

UL49.5 expression yields a type 1 transmembrane protein with a predicted size of 96 amino acids and an apparent molecular mass of 9 kDa. The protein can be detected at the cell surface and in the virion membrane (26). The UL49.5 polypeptide has a cleavable N-terminal signal peptide of 22 amino acids (18), a predicted extracellular domain of 32 amino acids, a transmembrane region of 25 amino acids, and a cytoplasmic tail of 17 amino acids (25). The extracellular domain of UL49.5 contains a cysteine residue that is highly conserved among

the UL49.5 homologs encoded by other members of the herpesvirus family. The UL49.5 protein can be coprecipitated with the TAP complex and may interact with the TAP1 and/or TAP2 proteins directly or through one of the other proteins in the MHC class I peptide-loading complex. The interaction of the UL49.5 protein with the TAP complex blocks conformational rearrangements in TAP required for peptide translocation into the endoplasmic reticulum (ER). In addition, UL49.5 induces degradation of the transporter and the UL49.5 protein itself (18). A truncated form of the UL49.5 protein lacking the cytoplasmic tail can still block the translocation of peptides, but it fails to trigger degradation of the TAP complex (18).

The BHV-1 UL49.5 protein is a homolog of the highly conserved glycoprotein N (gN) found in all herpesviruses studied to date (6). Like its homologs in several other species, the BHV-1 UL49.5 is not glycosylated (26). All gN homologs investigated so far form a complex with the transmembrane (glyco)protein M (gM) (8, 15, 21, 23, 30, 34, 39). The gN/gM complex is implicated in such processes as maturation of virions and control of membrane fusion (31, 32, 40). The immune evasion properties of UL49.5 have been found in several varicelloviruses, including pseudorabies virus and equine herpesvirus 1 in addition to BHV-1 (18).

The BHV-1 gM protein is encoded by the UL10 gene and is a type IIIa protein with a predicted size of 438 amino acids (National Center for Biotechnology Information database, accession number gi:9629818). It contains a proline-cysteine pair at amino acid positions 44 and 45 from the N terminus, in the first extracellular domain. This proline-cysteine pair is highly conserved within the gM homologs encoded by other members of the herpesvirus family. The BHV-1 gM-coding region has one predicted N-glycosylation site, located at the putative extracellular domain at amino acid residue 56 (39). The extracellular domain is followed by seven predicted hydrophobic domains separated by hydrophilic regions of 10 to 30 amino acids, consistent with a multiple-transmembrane domain (predicted using the TMHMM2 program). A putative cytoplasmic tail of 100 amino acids follows the putative transmembrane domain. The predominant gM protein found in BHV-1-infected cells and in BHV-1 virions has an apparent molecular mass of about 43 kDa (39). BHV-1 gM is a late protein that can first be detected 9 h postinfection (39). Both glycosylated and nonglycosylated gM can be coprecipitated with the UL49.5 protein from infected cells, and there is evidence that UL49.5 and gM are covalently linked by a disulfide bond (39). The UL49.5 protein can also form a disulfide-linked 15-kDa homodimer (26), but it seems to bind gM as a monomer (39). How many UL49.5 molecules react with the TAP complex is still unknown.

To study whether the complex formation between BHV-1 gM and UL49.5 has an effect on the inhibition of the TAP transporter, two approaches were followed. First, the assembly of UL49.5/gM complexes and TAP inhibition were studied using retrovirus-transduced cell lines constitutively expressing wild-type UL49.5 or UL49.5 mutants, together with gM. The second approach involved investigation of the UL49.5/gM complex formation and its effect on TAP inhibition in BHV-1-infected cells. It was found that UL49.5/gM association can indeed interfere with the inhibition of TAP. In BHV-1-infected cells, however, there appears to be sufficient non-gM-bound UL49.5 protein to surpass this interference.

Materials and Methods

Cells and viruses. Madin-Darby bovine kidney (MDBK) cells (American Type Culture Collection) and the human melanoma Mel JuSo cells (MJS; obtained from J. Neeffjes, The Netherlands Cancer Institute, Amsterdam) were grown in RPMI 1640 medium, supplemented with 10% fetal bovine serum, at 37°C in a 5% CO₂ humidified atmosphere. BHV-1 (Dutch field strain Lam) and its virion host shutoff (vhs) deletion mutant (19) were propagated and titrated on MDBK cells. BHV-1 infections were performed on MDBK or MJS cells as previously described (20).

Retroviral transduction. The construction of MJS cell lines, expressing wildtype BHV-1 UL49.5 or its mutated version lacking the cytoplasmic tail (UL49.5 Δ tail), was described elsewhere (18). MJS cells expressing the UL49.5 protein that misses both the cytoplasmic tail and the transmembrane region (UL49.5 Δ tail Δ TM) and MJS cells expressing BHV-1 gM or gM in combination with wild-type or truncated UL49.5 were made as follows. First, the coding region for UL49.5 Δ tail TM was amplified from the plasmid pCDNA3-IRES-NLS-GFPUL49.5 (18) using the following primers: forward, 5'-CAGAATTCACCATGC CGCGGTCCG-3'; reverse, 5'-AACGAATTCTCACTGCGGTGGCTCCG-3'. The obtained PCR product was inserted into the pLZRS-IRES-GFP retrovirus vector upstream of the internal ribosome entry site (IRES). The BHV-1 UL10 sequence encoding gM was amplified from purified BHV-1 Lam DNA using the following primers: forward, 5'-CACGAATTCATAGCA-3'; reverse, 5'-GGGG ATCCCGTCATGGCGGG-3'. The PCR product was inserted into the pLZRS retrovirus vector upstream of the IRES and the truncated nerve growth factor receptor-encoding sequence (pLZRS-IRES- Δ NGFR). PCRs were performed under standard conditions using *Pfu* DNA polymerase (Invitrogen). A single-amino-acid difference, Gly₂₄→Ala₂₄ (strain Lam), in gM was observed in comparison with the GenBank sequence (accession number gi:9629818). Recombinant retroviruses were obtained in the Phoenix amphotropic packaging system as described previously (http://www.stanford.edu/group/nolan/retroviral_systems/retsys.html). MJS or MJS-UL49.5 cells were transduced with recombinant retroviruses to generate the following cell lines: MJS gM, MJS UL49.5/gM, MJS UL49.5 Δ tail Δ TM, MJS UL49.5 Δ tail TM/gM, MJS UL49.5 Δ tail, and MJS UL49.5 Δ tail/gM. The GFP-positive and NGFR-positive cells were sorted using a FACSVantage cell sorter (Becton Dickinson).

Antibodies. The antibodies used in this study included two BHV-1 UL49.5 monospecific polyclonal rabbit sera raised against two synthetic peptides. The N-terminal peptide H11 (RDPLLDAMRREGAMDFWSAGCYARGVPLSEKK) was conjugated to glutathione S-transferase (GST) purified from the pGEX system according to the manufacturer's instructions (Amersham). The conjugation was performed with 0.05% glutaraldehyde (Sigma-Aldrich) according to the method described by Hancock et al. (11). The S-acetylmecaptoacetic acid (SAMA) group was coupled to the C-terminal peptide H19 (RLMGASGPNKESRGRG) as described previously (14). The SAMA peptide was subsequently conjugated to bromoacetylated GST (14). Rabbits were injected intradermally with the peptide-GST conjugates emulsified in Freund's complete adjuvant. At 3-week intervals, the rabbits received four additional subcutaneous immunizations with the conjugates emulsified in Freund's incomplete adjuvant. For the production of the polyclonal rabbit serum raised against the 63 C-terminal amino acids of BHV-1 gM, the recombinant gMC-63 construct was used (a kind gift of G. J. Letchworth, Agricultural Research Service, USDA, Laramie, WY) (39). Rabbits were immunized according to the protocol described above. A BHV-1 vhs-specific polyclonal rabbit serum was raised against a His-tagged UL41 protein produced in baculovirus and purified on Ni-tris-carboxymethyl ethylene diamine columns (A&A Biotechnology, Poland). gM- or UL49.5-specific mouse polyclonal sera used in immunoblotting detection of gM/UL49.5 in immunoprecipitates were a kind gift of G. J. Letchworth (39). Anti-TAP1 monoclonal antibody (MAb) 143.5 was kindly provided by R. Tampé (Institute of Biochemistry, The Johann Wolfgang Goethe University, Frankfurt, Germany), anti-TAP2 MAb 435.3 was a kind gift from P. van Endert (INSERM U25, Institute Necker, Paris, France), and anti-human MHC class I complex MAb W6/32 was kindly provided by H. Ploegh (Whitehead Institute/MIT, Cambridge, Mass.). Anti-BHV-1 gB MAb14 and anti-BHV-1 gC MAb71 were obtained from the Animal Sciences Group, Lelystad, The Netherlands. A monoclonal antibody directed against human beta-actin was purchased from Sigma-Aldrich.

Flow cytometry. Cell surface expression of specific molecules was determined by indirect immunofluorescence using primary antibodies as indicated and, as a second step, goat anti-mouse immunoglobulin (Ig)-phycoerythrin (Jackson Laboratories) (20). To determine the viability of the cells, a 1 μ l of 1 mg ml⁻¹ of 7-aminoactinomycin D (7-AAD; Calbiochem) was added to the cells 20 min prior to the analysis. Cells were analyzed using a FACSCalibur flow cytometer (Becton Dickinson) and CellQuest software.

Metabolic labeling, pulse-chase analysis, immunoprecipitations, and immunoblotting. Mock-infected or BHV-1-infected cells were metabolically labeled with [³⁵S]methionine/cysteine mix (200 μ Ci ml⁻¹; ³⁵S Redivue Promix; Amersham) for 35 min and lysed in a buffer containing 1% (wt/vol) digitonin (Calbiochem), 50 mM Tris-HCl, pH 7.5, 5 mM MgCl₂, 150 mM NaCl, 1 mM leupeptin, 1 mM 4-(2- aminoethyl) benzenesulfonyl fluoride (AEBSF), and 20 μ M Cbz-L3 (Peptides International, Inc.). After removal of cell nuclei and debris by centrifugation, aliquots of the cell lysates were precipitated with trichloroacetic acid, and radioactivity was measured. Samples with equal amounts of incorporated radioactivity were subjected to immunoprecipitation with anti-gM and anti-UL49.5 antibodies. Precipitates were treated at 56°C with sodium dodecyl sulfate-polyacrylamide gel electrophoresis (SDS-PAGE) sample buffer (2% SDS, 50 mM Tris pH 8.0, 10% glycerol, 0.05% bromophenol blue) under nonreducing or reducing conditions, i.e., in the absence or presence of 5% β -mercaptoethanol, respectively. The samples were separated on 13% SDS-polyacrylamide gels. The gels were exposed to phosphor imaging screens, which were scanned using a Personal Molecular Imager FX (Bio-Rad) and analyzed using Quantity One software (Bio-Rad).

Where indicated, the cells were infected with BHV-1 in the presence of phosphonoacetic acid (PAA; MP Biomedicals) at a concentration of 300 μ g ml⁻¹ to prevent late viral gene expression.

For immunoblotting analysis, the cells were lysed in NP-40 lysis mix containing 50 mM Tris-HCl, pH 7.4, 5 mM MgCl₂, and 0.5% NP-40, supplemented with 1 mM AEBSF, 1 mM leupeptin, and 20 μ M Cbz-L3. Lysates were incubated at 56°C in a reducing SDS-PAGE sample buffer, separated by SDS-PAGE, and blotted onto polyvinylidene difluoride membranes. The membranes were blocked overnight with 5% (wt/vol) skim milk in TBST (10 mM Tris-HCl, pH 8.0, 150 mM NaCl, 0.1% Tween 20), incubated for 60 min with anti-gM or anti-H11 serum diluted 1:500 in 3% milk-TBST, and, after extensive washing with TBST, reacted with peroxidase-labeled anti-rabbit antibody (1:2,000; DAKO). MAbs directed against TAP1, TAP2, or actin were used as previously described (18). Peroxidase-labeled anti-mouse antibody (1:1,000; DAKO) was used for the detection of the immune complexes using ECL Plus (Amersham).

gM was depleted from digitonin lysates of BHV-1-infected cells by three rounds of immunoprecipitation with anti-gM serum. The immune complexes were isolated with protein A/protein G-Sepharose (Amersham), and the lysates were clarified with Sepharose beads before the next round of immunoprecipitation. The gM-depleted lysate was used to immunoprecipitate UL49.5 as described above.

Analysis of N-linked glycosylation. Equivalent amounts of NP-40 cell lysates were incubated with endo- β -N-acetylglucosaminidase H (EndoH; New England Biolabs) or peptide: N-glycosidase F (PNGase F; Roche) according to the manufacturers' conditions. The reactions were terminated by the addition of SDS-PAGE sample buffer. The samples were separated by SDS-PAGE and analyzed by immunoblotting.

Immunofluorescence. MJS cells were grown on microcover glass, fixed with 4% paraformaldehyde in phosphate-buffered saline (PBS), and permeabilized with 0.2% Triton X-100 in PBS for 5 min. UL49.5 was detected with H11 anti-UL49.5 serum (1:8,000 dilution).

gM was stained with anti-gM serum (1: 5,000), *trans*-Golgi membranes were stained with anti-Golgin 97 MAbs (Molecular Probes; 1:200), and concanavalin A (ConA)-Alexa 488 conjugate (Molecular Probes; 1:10,000) was used as the ER and *cis*-Golgi marker. All antibody dilutions were prepared in PBS containing 1% bovine serum albumin (Sigma-Aldrich). Following three washes with PBS, the cells were incubated with secondary antibodies (1:3,000; Molecular Probes). gM and UL49.5 were visualized with Alexa 594-conjugated goat anti-rabbit IgG. Golgin 97 was visualized with Alexa 633-conjugated goat anti-mouse IgG. The blue signal was electronically converted into green after the analysis of the images using a Nikon ECLIPSE TE300 confocal laser scanning microscope.

Peptide transport assay. The fluorescein-labeled peptide transport assay was performed as previously described (18). Briefly, MJS cells were permeabilized with 2 IU ml⁻¹ of Streptolysin O (Murex Diagnostics Ltd.) at 37°C for 15 min. The cells (2 x 10⁶ cells/sample) were subsequently incubated with 20 µl (~30 pmol µl⁻¹) of the fluorescein-conjugated synthetic peptide CVNKTERAY in the presence or absence of 10 µl of 100 mM ATP at 37°C for 10 min. Peptide translocation was terminated by adding 1 ml of ice-cold lysis buffer containing 1% Triton X-100. After 20 min of lysis, cell debris was removed by centrifugation and supernatants were collected and incubated at 4°C for 1 h with 100 µl of concanavalin A (ConA)-Sepharose (Amersham) to isolate the glycosylated peptides. After extensive washing of the beads, the peptides were eluted with elution buffer (500 mM mannopyranoside, 10 mM EDTA, 50 mM Tris-HCl, pH 8.0) by rigorous shaking for 1 h at 25°C. Eluted peptides were further separated from ConA by centrifugation at 12,000 x g. The fluorescence intensity was measured using a fluorescence plate reader (CytoFluor, PerSeptive Biosystems) with excitation and emission wavelengths of 485 nm and 530 nm, respectively.

Results

BHV-1 UL49.5 forms a complex with gM outside the context of viral infection and is required for gM maturation. To study the influence of the UL49.5/gM complex formation on the inhibition of the TAP transporter, MJS cells expressing UL49.5 and capable of showing the TAP inhibition (18) were transduced with a recombinant retrovirus expressing gM. Two major forms of gM, with molecular masses of 36 and 45 kDa, respectively, were detected in the MJS UL49.5/gM cells (Fig. 1A, lane 6). These products resemble the forms of gM found in BHV-1-infected cells (Fig. 1A, lane 3), albeit with different ratios between the 36-kDa and 45-kDa species. The difference in mobility of the higher molecular mass forms of gM is due to an artifact in the gel. Treatment of the samples with PNGase F, which removes all N-linked glycans regardless of their maturation stage, revealed the gM protein backbone of about 34 kDa (lanes 2 and 5). Upon digestion with endoglycosidase H (EndoH), the 36-kDa species was lost, thus identifying this band as the immature form of gM (compare lanes 3 and 4 as well as lanes 6 and 7).

When gM was expressed in the absence of UL49.5, only the 36-kDa immature form could be detected (Fig. 1A, lane 9). This product was EndoH sensitive (lane 10), indicating that UL49.5 is required for maturation of gM. Coimmunoprecipitation experiments performed on MJS UL49.5/gM cells indicated that UL49.5 can indeed form a complex with gM outside the context of a viral infection (Fig. 1B). Staining of a gM immunoprecipitate with anti-UL49.5 antibodies revealed the coprecipitation of UL49.5 (Fig. 1B, lane 2, lower panel). Conversely, anti-UL49.5 antibodies coprecipitated gM (Fig. 1B, lane 3, upper panel).

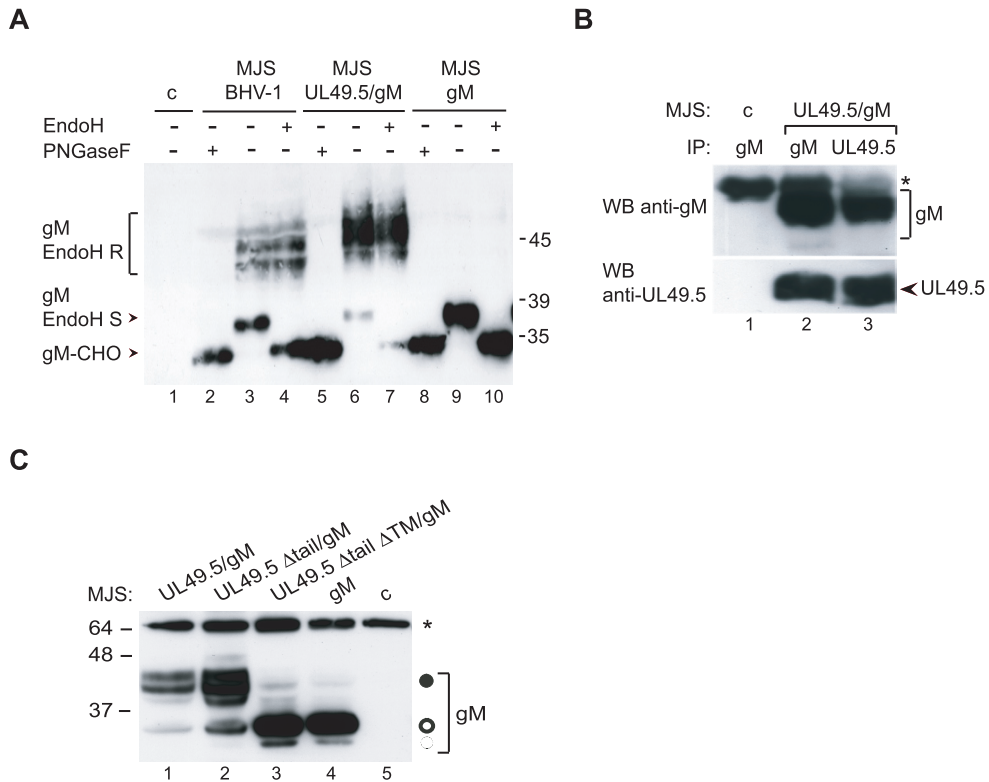


Fig. 1. UL49.5 is required for gM maturation. (A) Cell lysates of control MJS (c), BHV-1-infected MJS, and MJS stably expressing gM or UL49.5/gM were treated with endoglycosidase H (EndoH) (+) or left untreated (-). The EndoH-resistant forms (gM EndoH R), the EndoH-sensitive form (gM EndoH S), and the peptide:N-glycosidase F (PNGaseF)-treated, deglycosylated form of gM (gM-CHO) were detected by immunoblotting with gM-specific antibodies. (B) UL49.5 and gM form a complex in MJS UL49.5/gM cells. UL49.5 or gM was immunoprecipitated (IP) with specific rabbit antibodies from control (c) or UL49.5/gM-coexpressing cells. Immunoprecipitates were separated by SDS-PAGE and stained by immunoblotting (WB) with mouse antibodies against either gM (upper panel) or UL49.5. (C) The transmembrane region of UL49.5 is important for functional processing of gM. The mature gM (solid circle) could be detected by immunoblotting either in full-length UL49.5/gM-coexpressing or tailless UL49.5/gM-coexpressing MJS (MJS UL49.5 Δtail/gM). Coexpression of UL49.5 lacking both its tail and transmembrane region in MJS UL49.5 Δtail TM/gM cells resulted in impaired maturation of high-mannose gM (open circle), comparable to MJS gM-expressing cells. The 34-kDa gM precursor is indicated with a dashed circle. c, control MJS; *, immunoglobulin heavy chain. Size markers are in kilodaltons.

The transmembrane region of UL49.5 is important for functional processing of gM. To investigate which domain(s) of UL49.5 contributes to the processing of gM, its maturation was analyzed in MJS cells transduced with a gM-expressing retrovirus in combination with a second retroviral vector expressing one of the truncated forms of UL49.5 (Fig. 1C). Deletion of the cytoplasmic tail of UL49.5 did not influence processing of gM (lane 2). Coexpression of gM with a form of UL49.5 lacking the cytoplasmic tail and the transmembrane domain did not result in maturation of gM (Fig. 1C, lane 3). This result indicates that the transmembrane domain of UL49.5, in combination with its ER-luminal/extracellular domain, is required for proper maturation of gM.

Coexpression of UL49.5 and gM results in the redistribution of both proteins to the TGN. To study the influence of coexpression of gM and UL49.5 on their subcellular distribution, immunofluorescence-confocal laser scanning microscopy was performed on MJS, MJS gM, MJS UL49.5, and MJS UL49.5/gM cells. Colocalization with the *trans*-Golgi network (TGN) marker Golgin 97 was also investigated. The expression of the individual gM and UL49.5 proteins in the absence of their counterparts resulted in a dispersed granular staining pattern, reminiscent of intracellular membranes. No colocalization with the TGN could be observed (Fig. 2D to F and M to O). The localization of UL49.5 was in accordance with previous observations in MJS TAP1-GFP UL49.5-expressing cells (18). UL49.5-gM coexpression resulted in a redistribution of both proteins to the TGN, where they colocalized with Golgin 97 (Fig. 2G to I and P to R). Taken together, these data show that coexpression of UL49.5 and gM facilitates their transport to distal Golgi compartments and guides the UL49.5 protein away from the endoplasmic reticulum, the site of TAP inhibition.

gM influences the UL49.5-mediated inhibition of TAP. To study the consequences of the complex formation of UL49.5 and gM, three aspects of the UL49.5 interference with the MHC class I antigen presentation pathway were analyzed. First, peptide transport activity of TAP was measured in cells expressing UL49.5 in the absence or presence of gM. As reported before (18), the expression of UL49.5 alone results in an almost complete block of peptide translocation by TAP (Fig. 3A). Coexpression of gM with UL49.5 restored TAP activity to 85% of normal transport in control cells. Second, it was analyzed whether coexpression of gM had an effect on TAP degradation by UL49.5. To this end, steady-state levels of TAP1 and TAP2 proteins were compared in MJS UL49.5, MJS gM, MJS UL49.5/gM, and control MJS cells. Immunoblotting analysis revealed that gM counteracted the UL49.5-mediated degradation of TAP (Fig. 3B, compare lanes 2 and 4). The levels of both TAP proteins in UL49.5/gM cells appeared to be indistinguishable from those in the control cells (compare lanes 1 and 4). The gM protein alone had no effect on TAP stability (lane 3).

Third, the downregulation of surface MHC class I expression by UL49.5 was analyzed in the presence of gM. This analysis showed that the majority of the UL49.5/gM cells retained an unaffected cell surface level of MHC class I molecules (Fig. 3C, compare boldface histograms 2 and 3). The observed differences between the UL49.5-expressing and UL49.5-gM-coexpressing cells were not caused by reduced UL49.5 expression, as comparable levels of UL49.5 could be detected in both cell lines (Fig. 3D). These data show that gM can counteract the inhibitory effect of UL49.5 on the function and stability of the TAP transporter and, consequently, can restore cell surface expression of MHC class I molecules.

Kinetics of expression of UL49.5 and gM differ during BHV-1 infection. To further study the influence of gM on UL49.5, the kinetics of UL49.5 and gM synthesis was analyzed during BHV-1 infection. MJS or MDBK cells were infected with BHV-1 at a multiplicity of infection (MOI) of 10, and then the cells were collected at 0, 3, 5, 8, and 12 h postinfection (hpi) and metabolically labeled with [³⁵S]cysteine/methionine mix for 35 min. UL49.5 and gM were immunoprecipitated from the cell lysates. UL49.5 could be detected in MJS as early as 3 hpi (Fig. 4A, left panel) and continued to be detectable at all later time points postinfection. Coprecipitation of gM with UL49.5 was observed at 8 and 12 hpi (Fig. 4A, left panel). To assess the sensitivity of the UL49.5 and gM expression to phosphonoacetic acid (PAA), a DNA replication inhibitor that allows discrimination between the intermediate-early/early and late proteins (28), the cells were infected in the absence or presence of PAA. UL49.5 synthesis was not affected by PAA treatment. As a control, the early glycoprotein B (gB) and the late BHV-1 virion host shutoff (vhs) protein, a homolog of the HSV-1 UL41-encoded protein (36), were precipitated from the same lysates. PAA treatment only marginally affected the expression of gB and significantly inhibited the synthesis of the vhs protein (Fig. 4B).

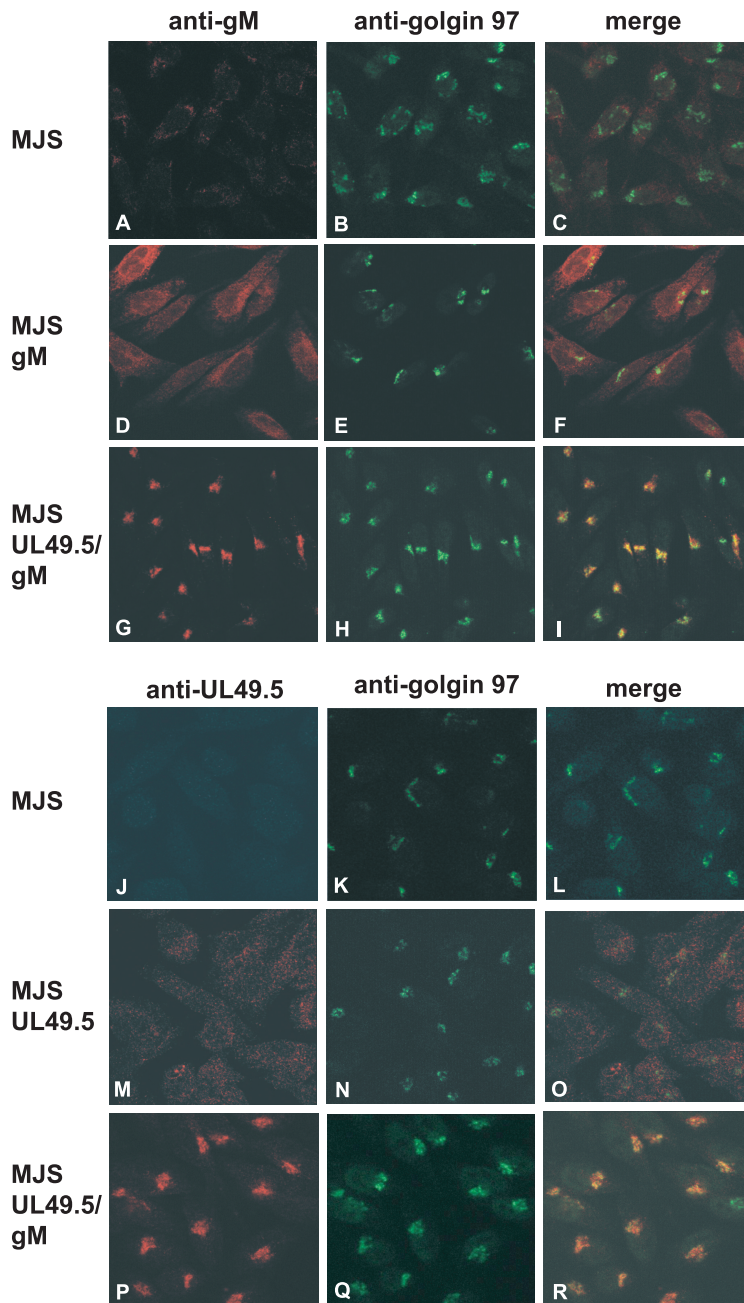


Fig. 2. Subcellular redistribution of UL49.5/gM analyzed by confocal laser scanning microscopy. gM was detected with gM-specific rabbit antibodies in MJS (A and C), MJS gM (D and F), or MJS UL49.5/gM (G and I). UL49.5 was detected with UL49.5-specific rabbit antibodies in MJS (J and L), MJS UL49.5 (M and O), or MJS UL49.5/gM (P and R). The trans-Golgi compartment was stained with MAb anti-Golgin 97 (B, E, H, K, N, and Q). The anti-gM and anti-UL49.5 rabbit antibodies were visualized with Alexa 594-conjugated goat anti-rabbit IgG. Golgin 97 was visualized with Alexa 633-conjugated goat anti-mouse IgG, and the signal was electronically converted into green. In the overlays, colocalization is shown in yellow.

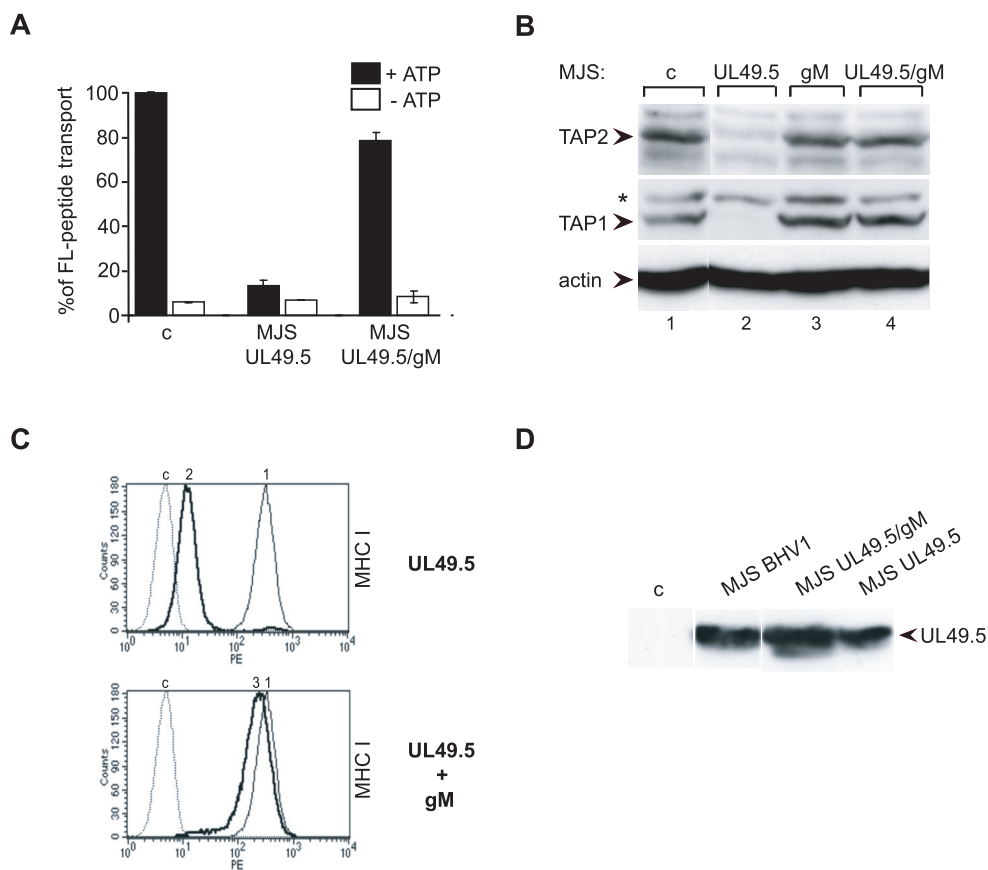


Fig. 3. gM interferes with UL49.5-mediated inactivation of TAP. (A) UL49.5 inhibition of TAP-dependent peptide transport is not observed in MJS UL49.5/gM cells. The translocation of fluorescent peptides in MJS UL49.5 or MJS UL49.5/gM cells is represented as a percentage of the translocation in control (c) MJS cells. FL, fluorescein. (B) UL49.5/gM coexpression results in the stabilization of TAP1 and TAP2 protein levels. Steady-state levels of TAP1, TAP2, and beta-actin were evaluated by immunoblotting in control (c) MJS, MJS UL49.5, MJS gM, or MJS UL49.5/gM cells using specific antibodies; *, unidentified background protein. (C) Downregulation of MHC class I surface expression by UL49.5 in the absence (upper panel, boldface line, no. 2) or in the presence of gM (lower panel, boldface line, no. 3). Thin line, MHC I in MJS cells (no. 1); dashed line, goat anti-mouse phycoerythrin control (c). (D) Immunoblot analysis of UL49.5 expression in MJS cells expressing UL49.5 or coexpressing UL49.5 and gM. Uninfected and BHV-1-infected MJS cells were included as controls.

Glycoprotein M species (45 kDa, 36 kDa, and 34 kDa) were detected in MJS cells late in infection (starting between 5 and 8 hpi; Fig. 4A, right panel), confirming previously published results (39). The 9-kDa protein coprecipitating with gM presumably represents UL49.5 (Fig. 4A, right panel). The synthesis of gM was blocked by PAA, which is typical for late proteins (28).

In the bovine MDBK cells, the interaction of UL49.5 and gM was observed as well (Fig. 4C). The early glycoprotein B and the late proteins gC and vhs were taken along as controls for PAA-mediated inhibition of late gene expression (Fig. 4D). Taken together, these data show that UL49.5 is produced as an early and late protein, whereas gM occurs as a late glycoprotein in BHV-1-infected cells. Both proteins were found to interact upon expression of gM at later stages of infection.

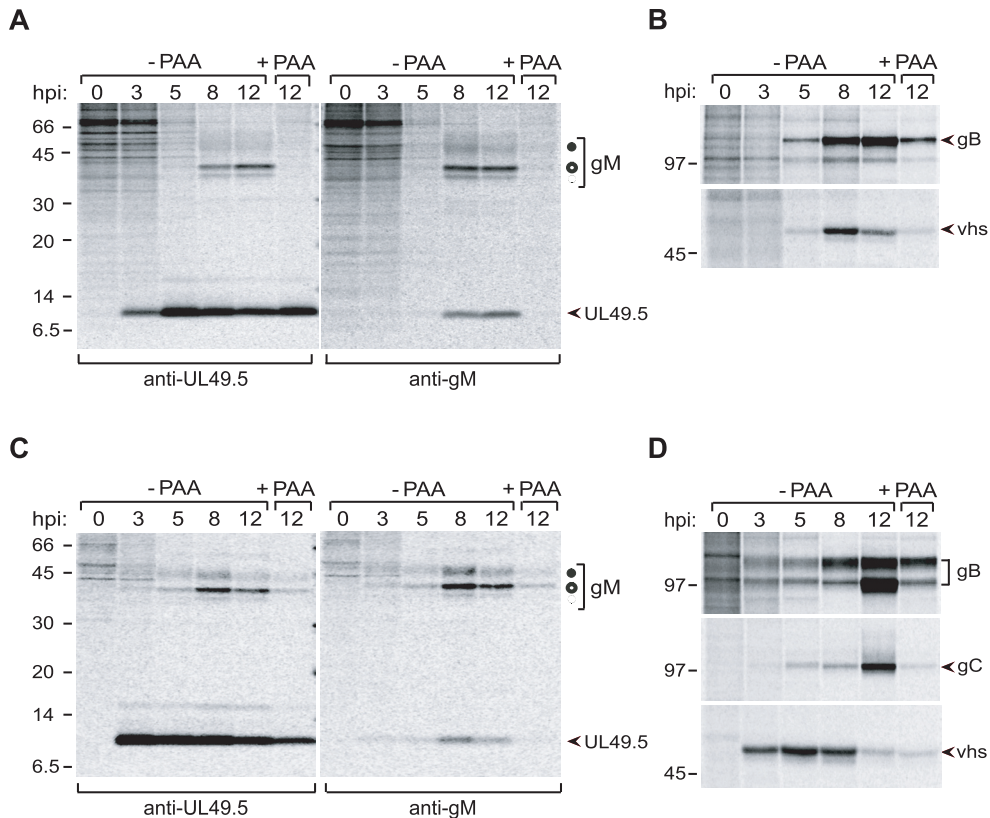


Fig. 4. UL49.5 and gM are expressed with different kinetics during BHV-1 infection. MJS cells were infected with BHV-1 in the absence or presence of phosphonoacetic acid (-PAA and +PAA, respectively), collected at the indicated time points postinfection (hpi), and metabolically labeled for 35 min. (A) UL49.5 (left panel) or gM (right panel) was immunoprecipitated from cell lysates with anti-UL49.5 and anti-gM antibodies, respectively. The fully glycosylated gM (solid circle), the high-mannose gM (open circle), and the gM precursor (dashed circle) are indicated. (B) The early glycoprotein B or the late virion host shutoff (vhs) protein were immunoprecipitated from the cell lysates as controls. (C) The experiment is the same as that described for panel A, performed in MDBK cells. (D) The early gB, the late gC, and the late vhs protein immunoprecipitated from the MDBK cell lysates. Size markers are in kilodaltons.

BHV-1 inhibits TAP-dependent peptide transport, also at late stages of infection.

Given the possibility that gM can counteract the inhibition of TAP by UL49.5, the observed interference with TAP function at early stages of infection with BHV-1 may be understandable on the basis of the late expression of gM. Knowing that gM synthesis occurs at later stages and results in UL49.5/gM complexes, TAP inhibition was studied in MJS cells infected with BHV-1 at 12 hpi. To exclude a potential virion host shutoff (vhs) effect on the synthesis of TAP or other components of the peptide-loading complex, peptide transport by TAP was evaluated in cells infected with either wild-type BHV-1 or a BHV-1 vhs deletion mutant. Under both conditions, a strong inhibition of TAP transport was observed (Fig. 5A), comparable to the inhibition observed during earlier times of infection (20). The UL49.5 protein and gM, detected in the tested cells by immunoblotting, are shown in Fig. 5B. As the vast majority of BHV-1-infected cells remained 7-AAD negative at 12 hpi (Fig. 5C), it was unlikely that the inhibition of TAP function was caused by reduced viability of the cells. These results indicate that TAP transport is efficiently blocked also at a late stage of infection, when both UL49.5 and gM are

present in the infected cells. Thus, it was concluded that the expression of gM at later stages of BHV-1 infection does not prevent inactivation of TAP.

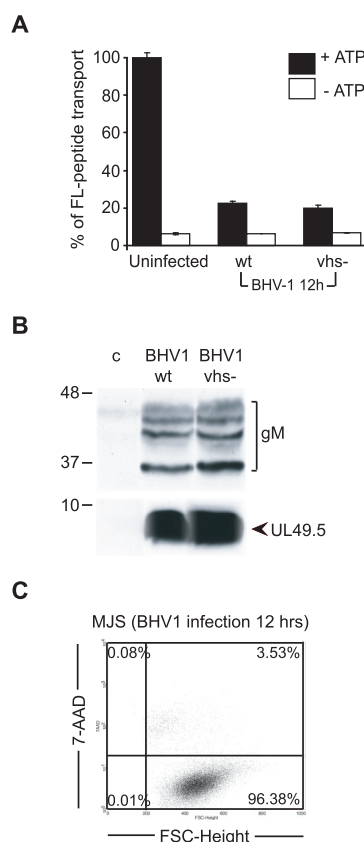


Fig. 5. BHV-1 inhibits ATP-dependent peptide transport by TAP at late stages of infection. MJS cells were infected with wild-type (wt) BHV-1 or a virion host shutoff deletion (vhs-) mutant for 12 h. (A) TAP-dependent peptide transport was assessed in the presence or absence of ATP using a fluorescein (FL)-tagged peptide. Uninfected MJS cells were used as a control. FL-peptide translocation in infected cells is represented as a percentage of the translocation in uninfected cells (set as 100%). (B) gM and UL49.5 detected in the BHV-1-infected cells used in the TAP transport assays shown in panel A. The cell lysates were separated by SDS-PAGE and analyzed by immunoblotting using antibodies against gM (upper panel) or UL49.5 (lower panel). Size markers are in kilodaltons. (C) The viability of the BHV-1-infected cells was evaluated at 12 hpi by 7-AAD staining and flow cytometry. FSC, forward scatter.

UL49.5 is produced in excessive amounts in BHV-1-infected cells, and only a proportion of it is incorporated into UL49.5-gM complexes. To investigate why gM does not counteract the inhibitory effect of UL49.5 on TAP in BHV-1-infected cells, the UL49.5/gM complex formation was studied in more detail during infection. The interaction between UL49.5 and gM is stabilized by a disulfide bridge between gM and the single cysteine within the ER-luminal/extracellular domain of UL49.5. Therefore, complex formation was evaluated under nonreducing conditions. MJS or MDBK cells were infected with BHV-1 at an MOI of 10, collected at 0, 2, 4, 6, and 10 hpi, and metabolically labeled with [³⁵S]cysteine/methionine for 35 min. UL49.5 was immunoprecipitated from digitonin lysates, and the resulting immune complexes were separated using nonreducing SDS-PAGE. At early stages of infection, UL49.5

was detected as a monomer and a dimer, migrating in the nonreducing gels at 9 and 15 kDa, respectively. Glycoprotein M was not present in these complexes, which is in agreement with the synthesis of UL49.5 prior to the production of gM in BHV-1-infected cells. The 15-kDa product was sensitive to reducing agents, indicating that it corresponds to dimers of UL49.5 (39). The UL49.5 monomers and dimers persist throughout infection, despite the synthesis of gM at later time points. Based on the electrophoretic mobility and endoglycosidase H digests (data not shown), it was possible to define the 48-kDa protein band as the mature gM-UL49.5 heterodimer, the 43-kDa band as the high-mannose gM-UL49.5 heterodimer, and the 39-kDa band as the precursor gM-UL49.5 heterodimer (Fig. 6A).

As an alternative approach to detect free UL49.5 protein in gM-expressing cells, UL49.5/gM complexes were first depleted by precipitation with excess of anti-gM antibodies in three consecutive rounds, followed by immunoprecipitation of the lysates with anti-UL49.5 antibodies. Only minute amounts of gM could be isolated from the gM-depleted cell lysates (Fig. 6B, lane 4). In contrast, UL49.5 could be precipitated in significant quantities from the depleted lysates (Fig. 6B, lane 5).

Also in BHV-1-infected MDBK cells, monomeric and dimeric UL49.5 was seen simultaneously with UL49.5/gM complexes when the experiment was performed under nonreducing conditions (Fig. 6C, lanes 10 and 11). The amounts of UL49.5/gM complexes isolated with either anti-gM or anti-UL49.5 antibodies were comparable, but the UL49.5-specific serum additionally yielded considerable quantities of monomeric and dimeric UL49.5. These results illustrate that the complex of gM and UL49.5 did not dissociate in the course of the experiment. If that had been the case, lower-molecularmass forms of gM would have been observed in the gM immunoprecipitates in addition to the UL49.5/gM complexes. This was not the case. This experiment indicates that significant quantities of free UL49.5 are present in infected cells, despite the expression of gM.

Immunofluorescence experiments were performed in BHV-1-infected cells to investigate whether the non-gM-associated UL49.5 can be detected in the ER. UL49.5 staining was observed in the ER and beyond (Fig. 7M to R), possibly in the TGN and transport vesicles. Glycoprotein M was detectable in the Golgi and post-Golgi compartments (Fig. 7D to I). The fact that UL49.5 could be detected in the ER when gM was expressed (10 and 14 hpi) supports the biochemical data indicating that UL49.5 remains capable of blocking TAP in the ER of BHV-1-infected cells despite the expression of gM.

Taken together, these results indicate that considerable amounts of free monomeric and dimeric UL49.5 protein are present in BHV-1-infected cells; only a proportion of the UL49.5 protein is engaged in UL49.5/gM complex formation.

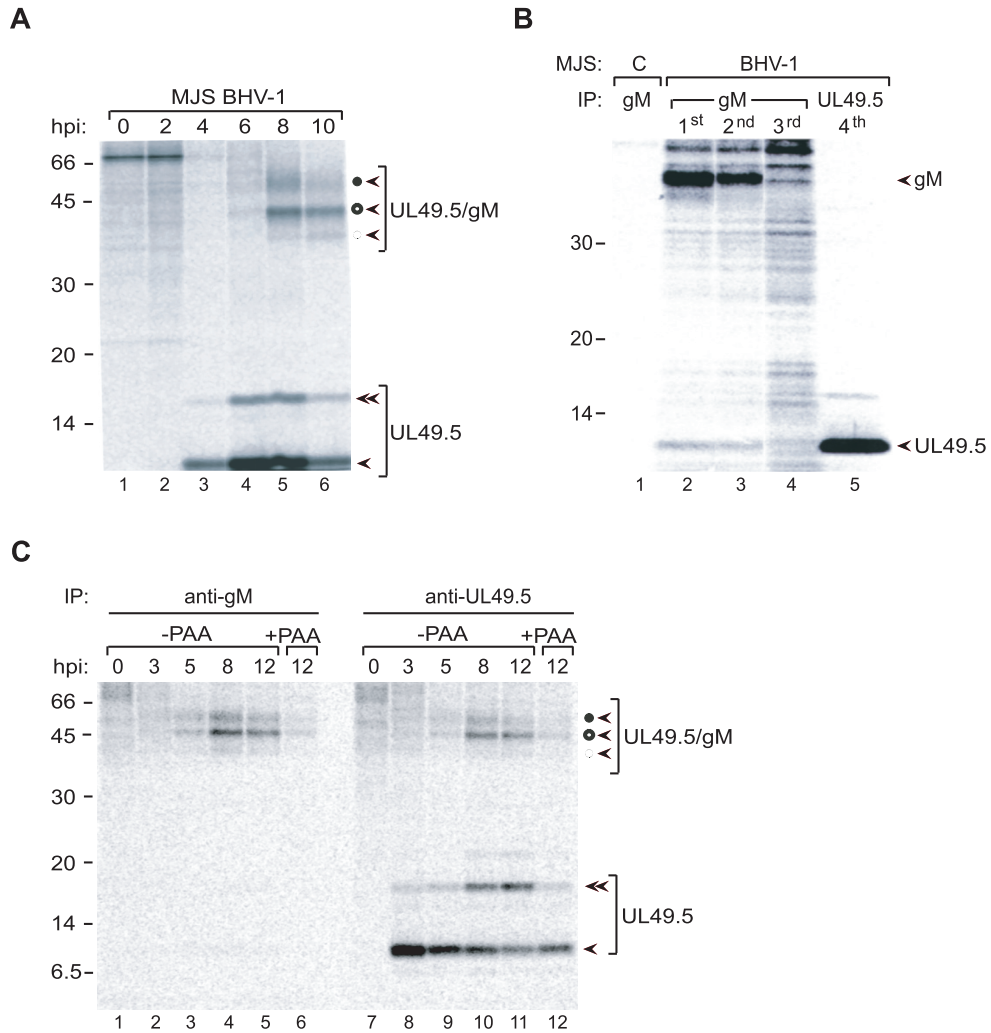


Fig. 6. UL49.5 is present in excess during BHV-1 infection. (A) BHV-1-infected MJS cells were collected at the indicated time points postinfection and metabolically labeled for 35 min. Cell lysates were subjected to immunoprecipitation with anti-UL49.5 antibodies and analyzed using nonreducing SDS-PAGE. Monomeric UL49.5 (solid arrow), UL49.5 dimers (double solid arrow), fully glycosylated gM-UL49.5 heterodimers (solid circle, solid arrow), high-mannose gM-UL49.5 heterodimers (open circle, solid arrow), and precursor gM-UL49.5 heterodimers (dashed circle, solid arrow) are indicated. (B) Mock-infected control cells (c) or BHV-1-infected cells were collected at 8.5 hpi and metabolically labeled for 30 min. Cell lysates were subjected to three sequential rounds of immunoprecipitation (IP) with anti-gM antibodies. After the third IP with gM, the lysate was subjected to a fourth, final IP with anti-UL49.5. (C) BHV-1-infected MDBK cells were collected at the indicated time points postinfection and metabolically labeled for 35 min. Cell lysates were subjected to immunoprecipitation with anti-gM (left panel) or anti-UL49.5 (right panel) antibodies and analyzed using nonreducing SDS-PAGE. Monomeric UL49.5, UL49.5 dimers, fully glycosylated gM-UL49.5 heterodimers, high-mannose gM-UL49.5 heterodimers, and precursor gM-UL49.5 heterodimers are indicated as for panel A. Size markers are in kilodaltons.

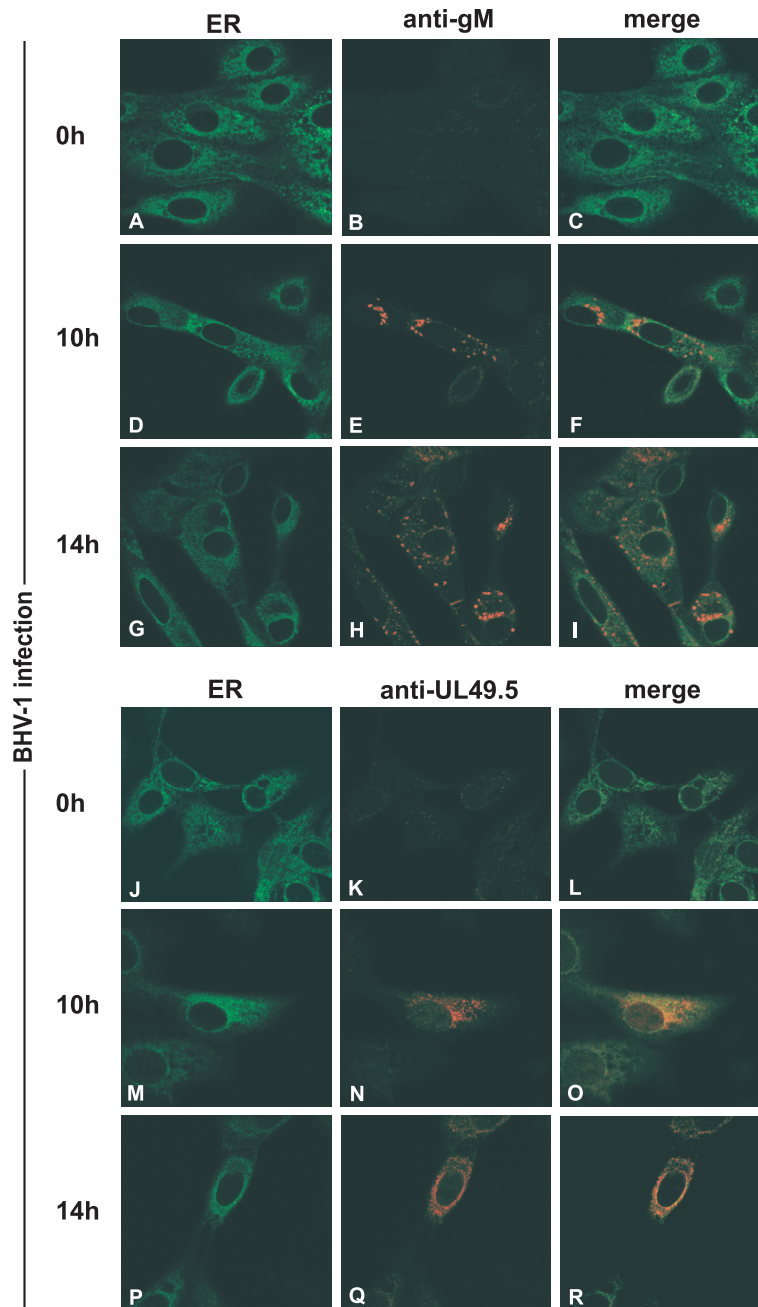


Fig. 7. Subcellular redistribution of UL49.5 and gM in BHV-1-infected MDBK cells, analyzed by confocal laser scanning microscopy. MDBK cells were infected with BHV-1 at an MOI of 1. gM was detected in infected cells with gM-specific rabbit antibodies at the indicated times postinfection (B, C, E, F, H, and I). UL49.5 was detected with UL49.5-specific rabbit antibodies (K, L, N, O, Q, and R). The ER/cis-Golgi was stained with concanavalin A-Alexa 488 (A, C, D, F, G, I, J, L, M, O, P, and R). The anti-gM and anti-UL49.5 rabbit antibodies were visualized with Alexa 594-conjugated goat anti-rabbit IgG. In the overlays, colocalization is shown in yellow.

Discussion

The study reported here was motivated by the recent identification of the BHV-1 UL49.5 protein as an inhibitor of the TAP transporter (18), in addition to its known interaction with gM, with which it forms a complex in infected cells (39). The heterodimer formation with another viral component makes UL49.5 unique among presently known herpesvirus-encoded TAP inhibitors, including the herpes simplex virus-encoded ICP47 (7, 13), the human cytomegalovirus-encoded US6 (1, 12, 24), and murine gammaherpesvirus 68-encoded mK3 (3, 4, 29). The latter inhibitors were described to occur in monomeric forms (1, 2, 22, 38). The interaction of gM with UL49.5 suggested that the former might act as a modulator of TAP inhibition by UL49.5. Hence, the UL49.5-mediated inactivation of TAP was studied in cells coexpressing gM. UL49.5 and gM appeared to form a complex outside the context of BHV-1 infection, indicating that no other viral (glyco)proteins are required for this interaction. The biochemical data presented in this study clearly indicate that UL49.5 is required for maturation of gM. Immunofluorescence-confocal laser scanning microscopy data support this conclusion. Whereas the individually expressed UL49.5 and gM proteins are retained in the ER, simultaneous expression of both proteins results in their transport to the *trans*-Golgi compartments. At present, it is unclear how UL49.5 influences the maturation of gM and promotes its egress from the ER. For the interaction of UL49.5 with the TAP complex, the cytoplasmic tail of UL49.5 is not needed (18). The extracellular domain and the transmembrane region of UL49.5 are sufficient to induce structural changes in the TAP complex that block its function. By analogy, these regions of UL49.5 are sufficient to mediate its interaction with gM. This arrangement may influence the conformation of gM and facilitate its export from the ER. Although not needed for the interaction with the TAP complex or for inhibition of peptide transport by TAP, the cytoplasmic tail of UL49.5 plays an essential role in the degradation of the TAP proteins by the proteasome (18).

Coexpression of UL49.5 and gM prevents the inhibition of TAP by UL49.5. As the UL49.5/gM complex formation results in its transport to the *trans*-Golgi compartment, this diminishes the pool of UL49.5 protein available for TAP inhibition in the ER. Whether at any stage during this competition the gM protein forms a part of the UL49.5-TAP complex is unclear. Attempts to show the presence of gM in immunoprecipitates of the TAP complex in BHV-1-infected cells have been unsuccessful (data not shown).

The studies performed in transduced cells were complemented with experiments in BHV-1-infected cells, in which the biosynthesis of UL49.5 and gM, as well as their interaction, was studied in a time-dependent fashion. The results show for the first time that UL49.5 of BHV-1 is expressed in the presence of PAA as an early protein and continues to be expressed as a late protein. In agreement with earlier observations (39), BHV-1 gM is a late protein. This creates a time window for UL49.5 to act on TAP without gM interference. Furthermore, our study indicates that when gM is expressed, only a fraction of UL49.5 is engaged in a complex with gM. Consequently, also at later stages of infection, sufficient gM-free UL49.5 protein is available to inhibit TAP effectively. This is in agreement with the observed TAP inhibition at 12 hpi.

The conservation of coding sequences for UL49.5/gN and gM homologs in the genomes of *Alpha*-, *Beta*-, and *Gammaherpesvirinae* for more than 200 million years suggests that these proteins have an important function in the life cycle of herpesviruses (6). All presently studied gN and gM homologs form a heterodimeric complex in which at least one partner is glycosylated (8, 15, 21, 23, 30, 34, 38). It is believed that this complex represents a functional unity and is implicated in virion maturation (23, 31, 35) and the control of membrane fusion (16, 17, 18). The inhibition of TAP by UL49.5 homologs seems to be a function that evolved more recently, as it could be demonstrated only for a number of varicelloviruses (18). The UL49.5 proteins of herpes simplex virus types 1 and 2 do not block TAP. The latter function is

performed by their respective ICP47 proteins (16–21). Also, beta- and gammaherpesviruses have developed other mechanisms to block TAP and evade cytotoxic T-cell recognition (27, 33).

Despite the inhibition of TAP and the downregulation of MHC class I cell surface expression, BHV-1 evokes a T-cell response in its host, implying that at some stage of infection, BHV-1 peptides are presented to the immune system. This has also been observed for other herpesviruses. Presumably, the immune evasion proteins delay recognition of the infected cells, thus creating a time window for undetected virus replication. In summary, under experimental conditions, BHV-1 gM can block the inhibition of the TAP transporter by UL49.5. In BHV-1-infected cells, however, this effect is not observed due to a temporal difference in UL49.5 and gM expression, combined with a relative overexpression of UL49.5.

Acknowledgements

We thank G. J. Letchworth for providing reagents. A.D.L. was supported by the FEBS Collaborative Experimental Scholarship for Central and Eastern Europe. D.K.-L. was supported by the Dutch Diabetes Research Foundation. This work was supported by grant no. 2 PO48 010 30 from the Ministry of Science and Education of Poland.

References

1. **Ahn K, Gruhler A, Galocha B, Jones TR, Wiertz EJ, Ploegh H, Peterson PA, Yang Y, Fruh K** (1997) The ER-luminal domain of the HCMV glycoprotein US6 inhibits peptide translocation by TAP. *Immunity* 6:613–621.
2. **Beinert D, Neumann L, Uebel S, Tampe R** (1997) Structure of the viral TAP-inhibitor ICP47 induced by membrane association. *Biochemistry* 36:4694–4700.
3. **Boname JM, de Lima BD, Lehner PJ, Stevenson PG** (2004) Viral degradation of the MHC class I peptide loading complex. *Immunity* 20:305–317.
4. **Boname JM, Stevenson PG** (2001) MHC class I ubiquitination by a viral PHD/LAP finger protein. *Immunity* 15:627–636.
5. **Cresswell P** (2000). Intracellular surveillance: controlling the assembly of MHC class I-peptide complexes. *Traffic* 1:301–305.
6. **Davison AJ, Dargan DJ, Stow ND** (2002) Fundamental and accessory systems in herpesviruses. *Antivir Res* 56:1–11.
7. **Fruh K, Ahn K, Djaballah H, Sempe P, van Endert PM, Tampe R, Peterson PA, Yang Y** (1995) A viral inhibitor of peptide transporters for antigen presentation. *Nature* 375:415–418.
8. **Fuchs W, Mettenleiter TC** (2005) The nonessential UL49.5 gene of infectious laryngotracheitis virus encodes an O-glycosylated protein which forms a complex with the non-glycosylated UL10 gene product. *Virus Res* 112:108–114.
9. **Gibbs EJJ, Rweyemamu MM** (1977) Bovine herpesviruses. *Vet Bull* 47:317–343.
10. **Gopinath RS, Ambagala APN, Hinkley S, Srikumar S** (2002) Effects of virion host shut-off activity of bovine herpesvirus 1 on MHC class I expression. *Viral Immunol* 15:595–608.
11. **Hancock DC, O'Reilly NJ, Evan GI** (1998) Synthesis of peptides for use as immunogens, p. 69–79. In J. D. Pount (ed.), *Methods in molecular biology*, vol. 80: immunochemical protocols, 2nd ed. Humana Press, Inc., New York, N.Y.
12. **Hengel H, Koopman JO, Flohr T, Muranyi W, Goulmy E, Hammerling GJ, Koszinowski UH, Momburg F** (1997) A viral ER-resident glycoprotein inactivates the MHC-encoded peptide transporter. *Immunity* 6:623–632.
13. **Hill A, Jugovic P, York I, Russ G, Bennink J, Yewdell P, Ploegh H, Johnson D** (1995) Herpes simplex virus turns off the TAP to evade host immunity. *Nature* 375:411–415.
14. **Hoogerhout P, Donders EMLM, van Gaans-van den Brink JAM, Kuipers B, Brugghe HF, Van Unen LMA, Timmermans HAM, ten Hove GJM, de Jong APJ, Peeters CAM, Wiertz EJHJ, Poolman JT** (1995) Conjugates of synthetic cyclic peptides elicit bactericidal antibodies against a conformational epitope on a class I outer membrane protein of *Neisseria meningitidis*. *Infect Immun* 63:3473–3478.
15. **Jons A, Dijkstra JM, Mettenleiter TC** (1998) Glycoproteins M and N of pseudorabies virus form a disulfide-linked complex. *J Virol* 72:550–557.
16. **Klupp BG, Nixdorf R, Mettenleiter TC** (2000) Pseudorabies virus glycoprotein M inhibits membrane fusion. *J Virol* 74:6760–6768.
17. **Konig P, Giesow K, Keil GM** (2002) Glycoprotein M of bovine herpesvirus 1 (BHV-1) is nonessential for replication in cell culture and is involved in inhibition of bovine respiratory syncytial virus F protein induced syncytium formation in recombinant BHV-1 infected cells. *Vet Microbiol* 86:37–49.
18. **Koppers-Lalic D, Reits EAJ, Rensing ME, Lipińska AD, Abele R, Koch J, Marcondes Rezende M, Admiraal P, van Leeuwen D, Bieńkowska-Szewczyk K, Mettenleiter TC, Rijsewijk FAM, Tampe R, Neeffjes J, Wiertz EJHJ** (2005). Varicelloviruses avoid T cell recognition by UL49.5-mediated inactivation of the transporter associated with antigen processing. *Proc Natl Acad Sci USA* 102:5144–5149.
19. **Koppers-Lalic D, Rijsewijk FAM, Verschuren SBE, van Gaans-van den Brink JAM, Neisig A, Rensing ME, Neeffjes J, Wiertz EJHJ** (2001) The UL41-encoded virion host shutoff (vhs) protein and vhs independent mechanisms are responsible for down-regulation of MHC class I molecules by bovine herpesvirus 1. *J Gen Virol* 82:2071–2081.
20. **Koppers-Lalic D, Rychlowski M, van Leeuwen D, Rijsewijk FAM, Rensing ME, Neeffjes JJ, Bieńkowska-Szewczyk K, Wiertz EJHJ** (2003) Bovine herpesvirus 1 interferes with TAP-dependent peptide transport and intracellular trafficking of MHC class I molecules in human cells. *Arch Virol* 148:2023–2037.
21. **Koyano S, Mar E-C, Stamey FR, Inoue N** (2003) Glycoproteins M and N of human herpesvirus 8 form a complex and inhibit cell fusion. *J Gen Virol* 84:1485–1491.

22. **Kyritsis C, Gorbulev S, Hutschenreiter S, Pawlitschko K, Abele R, Tampe R** (2001) Molecular mechanism and structural aspects of transporter associated with antigen processing inhibition by the cytomegalovirus protein US6. *J Biol Chem* 276:48031–48039.
23. **Lake CM, Molesworth SJ, Hutt-Fletcher LM** (1998) The Epstein-Barr virus (EBV) gN homolog BLRF1 encodes a 15-kilodalton glycoprotein that cannot be authentically processed unless it is coexpressed with the EBV gM homolog BBRF3. *J Virol* 72:5559–5564.
24. **Lehner PJ, Karttunen JT, Wilkinson GW, Cresswell P** (1997) The human cytomegalovirus US6 glycoprotein inhibits transporter associated with antigen processing-dependent peptide translocation. *Proc Natl Acad Sci USA* 94:6904–6909.
25. **Liang X, Chow B, Li Y, Raggo C, Yoo D, Attah-Poku S, Babiuk LA** (1995) Characterization of bovine herpesvirus 1 UL49 homolog gene and product: bovine herpesvirus 1 UL49 homolog is dispensable for virus growth. *J Virol* 69:3863–3867.
26. **Liang X, Chow B, Raggo C, Babiuk LA** (1996) Bovine herpesvirus 1 UL49.5 homolog gene encodes a novel viral envelope protein that forms a disulfide-linked complex with a second virion structural protein. *J Virol* 70:1448–1454.
27. **Lilley BN, Ploegh HL** (2005) Viral modulation of antigen presentation: manipulation of cellular targets in the ER and beyond. *Immunol Rev* 207:126–144.
28. **Ludwig GV, Letchworth GJ** (1987) Temporal control of bovine herpesvirus 1 glycoprotein synthesis. *J Virol* 61:3292–3294.
29. **Lybarger L, Wang X, Harris MR, Virgin HW4th, Hansen TH** (2003) Virus subversion of the MHC class I peptide-loading complex. *Immunity* 18:121–130.
30. **Mach M, Kropff B, Dal Monte P, Britt W** (2000). Complex formation by human cytomegalovirus glycoproteins M(gpUL100) and N(gpUL73). *J Virol* 74:11881–11892.
31. **Mettenleiter TC** (2000) Aujeszky's disease (pseudorabies) virus: the virus and molecular pathogenesis—state of the art. *Vet Res* 31:99–115.
32. **Osterrieder N, Neubauer A, Brandmuller C, Braun B, Kaaden OR, Baines JD** (1996) The equine herpesvirus 1 glycoprotein gp21/22a, the herpes simplex virus type 1 gM homolog, is involved in virus penetration and cell-to-cell spread of virions. *J Virol* 70:4110–4115.
33. **Ressing ME, Keating SE, van Leeuwen D, Koppers-Lalic D, Papworth IY, Wiertz EJ, Rowe M** (2005) Impaired transporter associated with antigen processing-dependent peptide transport during productive EBV infection. *J Immunol* 174:6829–6838.
34. **Rudolph J, Seyboldt C, Granzow H, Osterrieder N** (2002) The gene 10 (UL49.5) product of equine herpesvirus 1 is necessary and sufficient for functional processing of glycoprotein M. *J Virol* 76:2952–2963.
35. **Seyboldt C, Granzow H, Osterrieder N** (2000) Equine herpesvirus 1 (EHV-1) glycoprotein M: effect of deletions of transmembrane domains. *Virology* 278:477–489.
36. **Smibert CA, Johnson DC, Smiley JR** (1992) Identification and characterization of the virion-induced host shutoff product of herpes simplex virus gene UL41. *J Gen Virol* 73:467–470.
37. **van Endert PM, Saveneau L, Hewitt EW, Lehner P** (2002) Powering the peptide pump: TAP crosstalk with energetic nucleotides. *Trends Biochem Sci* 27:454–461.
38. **Wang X, Lybarger L, Connors R, Harris MR, Hansen TH** (2004) Model for the interaction of gammaherpesvirus 68 RING-CH finger protein mK3 with major histocompatibility complex class I and the peptide-loading complex. *J Virol* 78:8673–8686.
39. **Wu SX, Zhu X P, Letchworth GJ** (1998) Bovine herpesvirus 1 glycoprotein M forms a disulfide-linked heterodimer with the U(L)49.5 protein. *J Virol* 72:3029–3036.
40. **Ziegler C, Just FT, Lischewski A, Elbers K, Neubauer A** (2005) A glycoprotein M-deleted equid herpesvirus 4 is severely impaired in virus egress and cell-to-cell spread. *J Gen Virol* 86:11–21.